

# SCIENTIFIC REPORTS



OPEN

## Nonerythropoietic Erythropoietin-Derived Peptide Suppresses Adipogenesis, Inflammation, Obesity and Insulin Resistance

Received: 13 November 2014

Accepted: 18 September 2015

Published: 13 October 2015

Yuqi Liu, Bangwei Luo, Rongchen Shi, Jinsong Wang, Zongwei Liu, Wei Liu, Shufeng Wang & Zhiren Zhang

Erythropoietin (EPO) has been identified as being crucial for obesity modulation; however, its erythropoietic activity may limit its clinical application. EPO-derived Helix B-surface peptide (pHBSP) is nonerythropoietic but has been reported to retain other functions of EPO. The current study aimed to evaluate the effects and potential mechanisms of pHBSP in obesity modulation. We found that pHBSP suppressed adipogenesis, adipokine expression and peroxisome proliferator-activated receptor  $\gamma$  (PPAR $\gamma$ ) levels during 3T3-L1 preadipocyte maturation through the EPO receptor (EPOR). In addition, also through EPOR, pHBSP attenuated macrophage inflammatory activation and promoted PPAR $\gamma$  expression. Furthermore, PPAR $\gamma$  deficiency partly ablated the anti-inflammatory activity of pHBSP in macrophages. Correspondingly, pHBSP administration to high-fat diet (HFD)-fed mice significantly improved obesity, insulin resistance (IR) and adipose tissue inflammation without stimulating hematopoiesis. Therefore, pHBSP can significantly protect against obesity and IR partly by inhibiting adipogenesis and inflammation. These findings have therapeutic implications for metabolic disorders, such as obesity and diabetes.

Obesity is a global and persistent growing health epidemic, whose incidence has almost doubled during the last 30 years<sup>1,2</sup>. Increased energy intake or decreased energy expenditure will lead to a massive increase in adipose tissue<sup>3</sup>, increasing the risk of type 2 diabetes (T2D) and other chronic diseases<sup>4</sup>. The prevention of obesity involves both dietary factors and physical activities; however, the incidence of obesity is still rising, suggesting that more attention should be focused on discovering new therapies<sup>5</sup>.

Obesity involves the formation of new adipocytes from precursor cells (adipocyte hyperplasia) and an increase in adipocyte size (adipocyte hypertrophy). In addition, adipocytes also secrete a variety of fatty acids and adipokines when they increase in size, which are closely associated with obesity-associated chronic diseases, such as T2D and cardiovascular disease<sup>6</sup>. Adipocyte hypertrophy is the main cause of adult-onset obesity, whereas adipocyte hyperplasia can be observed in children and morbidly obese adults<sup>7</sup>. Therefore, the modulation of adipocyte hypertrophy and hyperplasia can be important for obesity intervention<sup>8</sup>.

Obesity is usually related to a chronic, low-grade inflammatory response, which is initiated by excess nutrients in metabolic cells and eventually exacerbated by further activation of specialized immune cells<sup>9</sup>. Growing evidence has established the causative links between obesity-induced inflammation and obesity-related insulin resistance (IR)<sup>10</sup>. For example, the proinflammatory cytokine TNF- $\alpha$  has been proven to mediate obesity-induced IR in rodents, and the chemokine monocyte chemoattractant protein-1 (MCP-1) has been demonstrated to impair adipocyte insulin sensitivity<sup>11,12</sup>. Many cells are involved in

Institute of Immunology, Third Military Medical University, 30 Gaotanyan Main Street, Chongqing 400038, People's Republic of China. Correspondence and requests for materials should be addressed to Z.Z. (email: zhangzhiren@yahoo.com)

obesity-associated inflammation, among which macrophages play an essential role. Adipose tissue macrophages (ATMs) comprise almost 40% of the immune cells in obese adipose tissue, playing key roles in regulating systemic IR, glucose tolerance and the development of metabolic dysfunction<sup>13</sup>. Obesity induces the activation of proinflammatory signaling in ATMs, resulting in upregulation of pro-inflammatory cytokines (i.e., TNF- $\alpha$ , IL-6 and inducible nitric oxide synthase (iNOS)), which act locally, contributing to IR<sup>14</sup>. Furthermore, the inhibition of inflammatory pathways in obesity has beneficial effects on insulin sensitivity in mouse models and human trials<sup>15–17</sup>.

Erythropoietin (EPO) is a pleiotropic hormone that regulates the production of red blood cells by binding to homodimer EPO receptor (EPOR<sub>2</sub>) and has been widely employed to treat anemia<sup>18</sup>. Moreover, a growing number of studies have reported EPOR expression in different cells, such as adipocytes, macrophages, neurons, endothelial cells and cardiac cells<sup>19–22</sup>. In adipocytes, EPO has been found to decrease preadipocyte differentiation, and mice with adipocyte-specific deletion of EPOR exhibited obesity and decreased glucose tolerance and insulin sensitivity<sup>23</sup>. In macrophages, EPO attenuates LPS-induced expression of IL-6 and TNF- $\alpha$ <sup>9</sup>. More importantly, exogenous EPO has been deemed to improve obesity and IR, indicating that EPO is a potent regulator of obesity<sup>24</sup>. However, EPO can induce erythropoiesis, and its long-term application may cause side effects, such as increasing hematocrit, raising blood pressure and increasing the risk of thrombosis, which limit its long-term clinical application<sup>25</sup>. Fortunately, an increasing number of studies have revealed that the tissue-protective function of EPO is induced via the activation of the EPOR-CD131 complex, the so-called tissue-protective receptor (TPR), whose affinity for EPO is 100 times lower than that of the homodimer EPOR<sub>2</sub><sup>26</sup>. Additionally, EPO analogues that are reported to maintain the tissue-protective properties of EPO while lacking erythropoietic potential have been developed.

EPO is determined to interact with (EPOR)<sub>2</sub> through its 3D structure (helix A, C and D). However, helix B is considered to exert the selective tissue-protective features of EPO. pHBSBP is an EPO Helix B-derived short peptide of 11 amino acids in length, which was reported to have no erythropoietic activity while retaining the tissue-protective properties of EPO and selectively binding to the EPOR-CD131 complex<sup>27,28</sup>. To better understand this EPO analogue, we constructed a stick model of pHBSBP (Supplementary Figure 1). Although pHBSBP has a short plasma half-life of several minutes, its protective effects in animals and humans can last over hours to days, indicating a rapid passage of pHBSBP into affected compartments and a rapid activation of TPR, leading to the sustained activation of related signal pathways, such as the PI3K/Akt axis<sup>29</sup>. Recently, pHBSBP has been reported to promote recovery from various diseases, such as burn injury, stroke, wound healing, renal ischemia/reperfusion, autoimmune diseases and status epilepticus, and it has also been reported to improve diet-induced IR. In addition, accumulated results from preclinical toxicological studies have raised no safety concerns regarding the application of pHBSBP<sup>30–34</sup>. However, the long-term effects and potential mechanisms of pHBSBP on obesity, IR and inflammation are not fully understood. Therefore, in the current study, we investigated the effects and potential mechanisms of pHBSBP on obesity regulation.

## Results

**pHBSBP inhibits adipogenesis in 3T3-L1 preadipocytes through TPR.** Mitotic clonal expansion (MCE) is a synchronous process involved in adipogenesis. 3T3-L1 preadipocytes synchronously reenter the cell cycle and undergo MCE after differentiation<sup>35</sup>. Therefore, we first examined whether pHBSBP can inhibit MCE by suppressing cell cycle progression in 3T3-L1 preadipocytes. As shown in Fig. 1A,B, undifferentiated 3T3-L1 cells did not undergo cell cycle progression until 8 days following treatment with isobutylmethylxanthine, dexamethasone and insulin (MDI), and pHBSBP intervention dose-dependently blocked the progression of 3T3-L1 preadipocytes at the G2 phase, suggesting that pHBSBP can suppress 3T3-L1 preadipocyte cell cycle progression. Moreover, the suppression of preadipocyte cell cycle progression may affect adipocyte differentiation. Therefore, we used an oil red O (ORO) staining experiment to detect adipocyte differentiation and found that MDI-mediated lipid and triglyceride accumulation in 3T3-L1 cells were dose-dependently reduced by pHBSBP (Fig. 1C,  $p < 0.005$  for doses 200, 100 and 50 nM; Fig. 1D,  $p < 0.01$  for doses 200, 100 and 50 nM), indicating that pHBSBP suppressed adipocyte differentiation.

Increased glucose metabolism is crucial for lipid and triglyceride accumulation. Therefore, we detected the activation of Akt, a key molecule that regulates the translocation of GLUT4 and further increases glucose uptake<sup>36</sup>. As shown in Fig. 1G, pHBSBP dose-dependently up-regulated Akt phosphorylation, suggesting that pHBSBP may increase glucose intake in 3T3-L1 cells ( $p < 0.05$ ).

PPAR $\gamma$  is a master regulator of adipogenesis in adipocytes; therefore, we further monitored the effect of pHBSBP on PPAR $\gamma$  expression in adipocytes. As shown in Fig. 1E,F, the mRNA and protein levels of PPAR $\gamma$  in 3T3-L1 preadipocytes were attenuated by pHBSBP in a dose-dependent manner ( $p < 0.01$ ).

Because a series of IR-related, pro-inflammatory adipokines are synthesized during adipocyte maturation, we further investigated the effects of pHBSBP on the expression levels of select adipokines in 3T3-L1 preadipocytes and found that pHBSBP dose-dependently down-regulated the mRNA levels of TNF- $\alpha$ , IL-6 and MCP-1 in MDI-induced 3T3-L1 preadipocytes (Fig. 2A–C,  $p < 0.05$ ).

To determine whether pHBSBP functions through TPR signaling in adipocytes, a reported EPOR antagonist, EPO mimetic peptide-9 (EMP9), was used<sup>37</sup>. Based on the results of a dose-response assay, 0.5 mg/mL EMP9 was used for the following experiments (Supplementary Figure 2). Co-treatment with EMP9

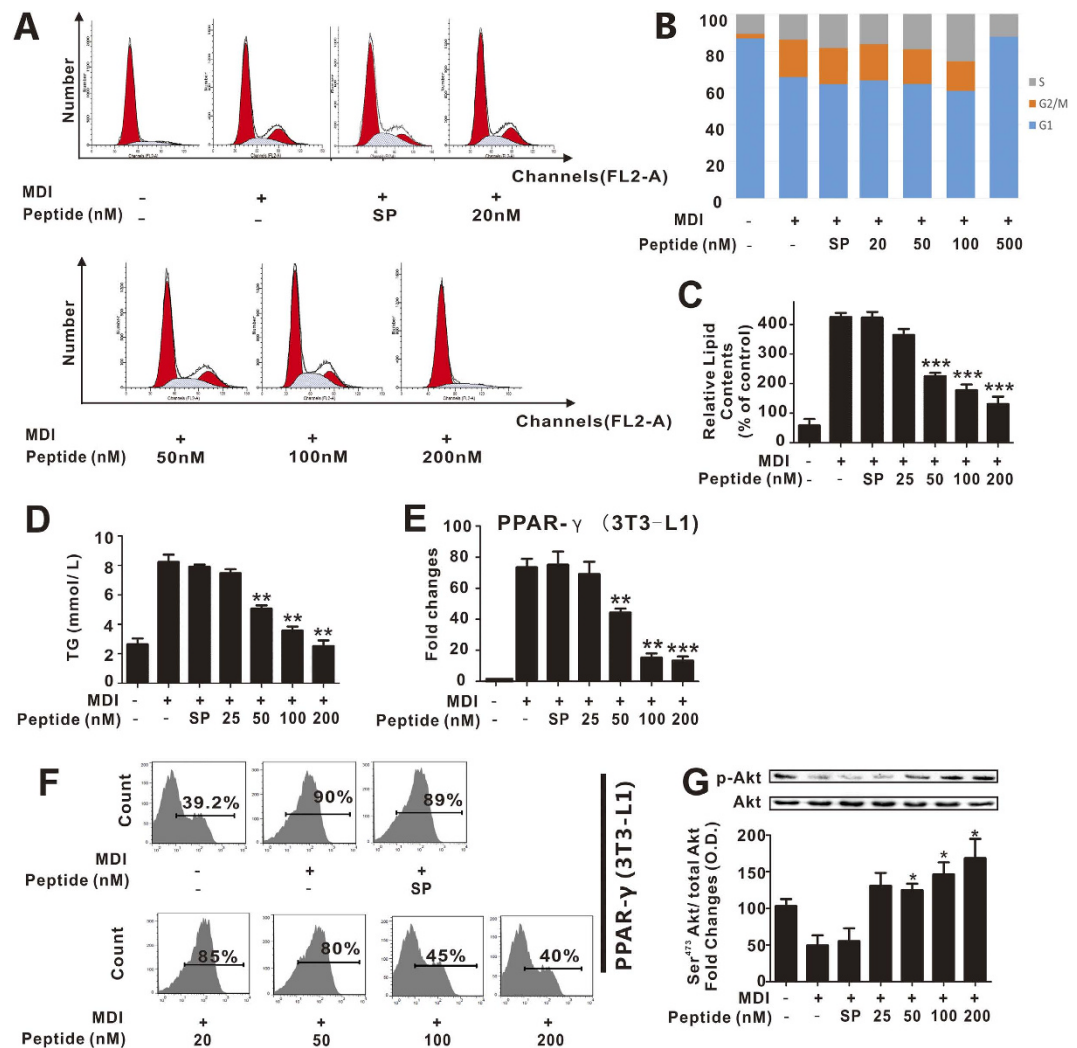


**Figure 1. pHBSP suppressed adipogenesis in 3T3-L1 cells.** Undifferentiated cells were induced to differentiate into mature 3T3-L1 pre-adipocytes by MDI treatment for 24 hours followed by insulin supplementation. At 24 hours, a subset of cells was used to test MCE, and the remaining cells were used at day 8 to test cell differentiation and expression of PPAR $\gamma$  mRNA. (A,B) Effects of pHBSP on MDI-induced cell cycle progression in 3T3-L1 preadipocytes. (C) pHBSP inhibited lipid storage, as shown by staining with oil red O solution. (D) pHBSP decreased the storage of triglyceride in 3T3-L1 cells. (E,F) pHBSP diminished the mRNA (E) and protein (F) levels of PPAR $\gamma$ . (G) pHBSP increased the phosphorylation of Akt in 3T3-L1 cells. N = 6 per group; TG indicates triglycerides, and SP indicates scrambled peptide; data are the mean  $\pm$  SEM; error bars indicate s.e.m., and significance is indicated by \* $p < 0.05$ , \*\* $p < 0.01$  and \*\*\* $p < 0.005$ , as determined by one-way analysis of variance followed by Dunnett's multiple comparison test.

abolished the anti-adipogenesis, anti-adipokine and PPAR $\gamma$ -suppressive effects of pHBSP in 3T3-L1 cells (Fig. 2D–I,  $p < 0.05$ ), indicating a TPR-dependent effect of pHBSP in 3T3-L1 cells.

**pHBSP inhibits pro-inflammatory cytokine expression in macrophages through TPR.** Subsequently, we tested the effects of pHBSP on the inflammatory activation of macrophages. As shown in Fig. 3A–F, pHBSP dose-dependently suppressed LPS-induced increases in iNOS, IL-6 and TNF- $\alpha$  mRNA levels in RAW264.7 macrophages and peritoneal macrophages. Interestingly, in contrast to adipocytes, in RAW264.7 macrophages, pHBSP dose-dependently increased the mRNA and protein levels of PPAR $\gamma$  (Fig. 3G,H,  $p < 0.05$ ). Furthermore, pHBSP dose-dependently induced PPAR $\gamma$  mRNA levels in peritoneal macrophages (Fig. 3I,  $p < 0.05$ ). In macrophages, the nuclear receptor PPAR $\gamma$  modulates cytokine expression; therefore, we next explored whether pHBSP exerted its anti-inflammatory function via PPAR $\gamma$  in macrophages. We found that in PPAR $\gamma$ -knockdown peritoneal macrophages, the effect of pHBSP on iNOS expression was abolished; however, the effects of pHBSP on TNF- $\alpha$  and IL-6 expression remained unchanged (Fig. 3J–L,  $p < 0.05$ ), indicating that the suppressive effect of pHBSP on macrophage inflammatory activation was partly due to its promotion of PPAR $\gamma$  expression.

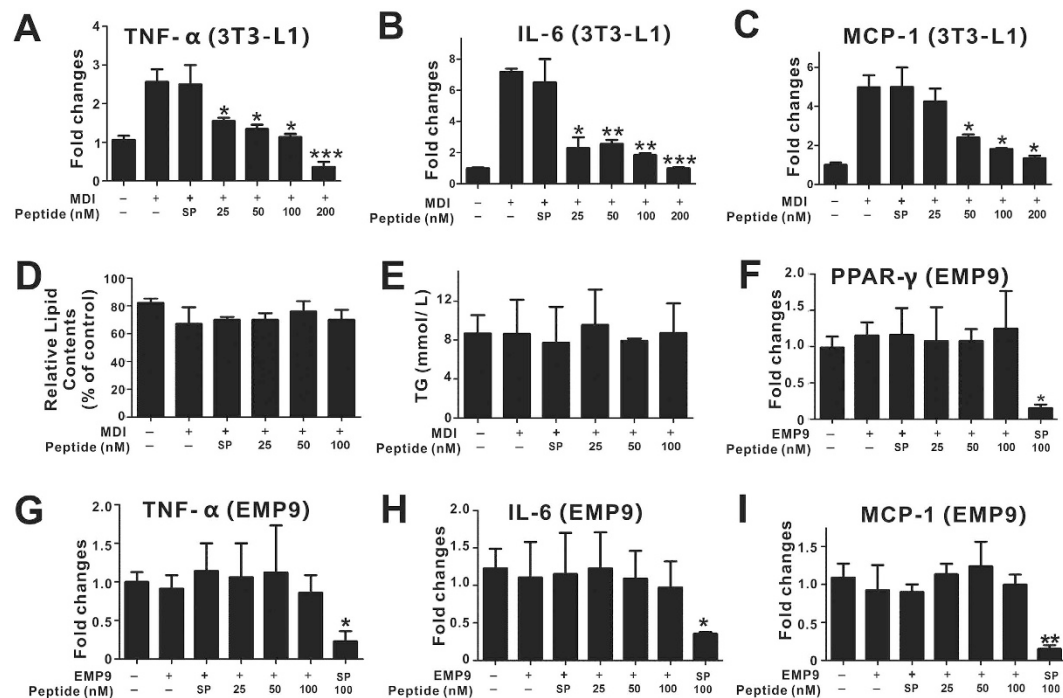


**Figure 2. pHBSP suppressed adipokine expression in 3T3-L1 cells.** Undifferentiated cells were induced to differentiate into mature 3T3-L1 pre-adipocytes by treating with MDI for 24 hours, and cells at day 8 were used to test the expression of adipokine mRNA. (A–C) pHBSP diminished the expression of TNF- $\alpha$  (A), IL-6 (B) and MCP-1 (C) mRNA in 3T3-L1 cells. (D–E) Administration of 0.5 mg/mL EMP9 counteracted the effects of pHBSP on differentiation of (D) and triglyceride accumulation (E) in 3T3-L1 preadipocytes. (F–I) Administration of 0.5 mg/mL EMP9 counteracted the effects of pHBSP on PPAR $\gamma$  (F), TNF- $\alpha$  (G), IL-6 (H) and MCP-1 (I) expression in 3T3-L1 cells. N = 6 per group; TG indicates triglycerides, and SP indicates scrambled peptide; data are the mean  $\pm$  SEM; the error bars indicate s.e.m., and significance is indicated by \* $p < 0.05$ , \*\* $p < 0.01$  and \*\*\* $p < 0.005$ , as determined by one-way analysis of variance followed by Dunnett's multiple comparison test.

Because Akt activation is involved in the activation of macrophages, we next evaluated Akt phosphorylation in macrophages following pHBSP stimulation. As shown in Fig. 4M, pHBSP dose-dependently increased Akt phosphorylation ( $p < 0.05$ ).

In addition, we investigated whether pHBSP inhibits macrophage inflammatory activation through TPR. As shown in Fig. 3N–Q, EMP9 deprived the anti-inflammatory and PPAR $\gamma$ -inducing functions of pHBSP in macrophages ( $p < 0.05$ ).

The down-regulation of pro-inflammatory cytokine expression implicates that pHBSP may tether the M1 polarization in macrophages; therefore, we further analyzed whether pHBSP can promote M2 polarization in macrophages. We found that co-treatment with pHBSP increased the expression of Fizz1, Arginase-1 and PPAR $\gamma$  compared to treatment with IL-4 alone (Fig. 4A–E,  $p < 0.05$ ), which was deprived by EMP9 (Fig. 4F–G,  $p < 0.05$ ).

### pHBSP attenuates high-fat diet (HFD)-induced obesity and IR without stimulating hematopoiesis.

Due to the potent anti-adipogenic and anti-inflammatory effects of pHBSP *in vitro*, we next explored pHBSP's effects on obesity and IR *in vivo*. HFD was used to induce obesity in mice by administering varying doses of pHBSP (120, 90, 60 and 30  $\mu$ g/kg) every other day from the beginning of HFD administration. At week 16, we found that HFD induced greater obesity ( $45.33 \pm 1.04$ g) than normal diet in mice ( $28.42 \pm 1.45$ g, Fig. 5A,  $p < 0.05$ ). Indeed, pHBSP dose-dependently reduced body weight in mice with HFD-induced obesity (Fig. 5A,  $p < 0.05$ ); food intake was also decreased by pHBSP in mice with diet-induced obesity (DIO) (Fig. 5B,  $p < 0.05$ ). Furthermore, pHBSP decreased fat mass in DIO mice by up to  $3.36 \pm 0.42$ g (Fig. 5C,  $p < 0.01$ ) but did not cause significant changes in lean body mass (Fig. 5D,  $P > 0.05$ ). Next, quantitative analysis of fat-pad weight disclosed that pHBSP treatment significantly decreased abdominal (49.34%, Fig. 5E,  $p < 0.05$ ) and subcutaneous adipose weight (52.65%, Fig. 5F,  $p < 0.05$ ) in DIO mice. Moreover, histological examination of epididymal white adipose tissue (WAT) revealed that the administration of pHBSP significantly reduced adipocyte size compared with that in a vehicle control group (Fig. 5G–K,  $p < 0.05$ ). Moreover, ORO staining showed that pHBSP diminished lipid storage in adipose tissue (Fig. 5L,  $p < 0.01$ ).

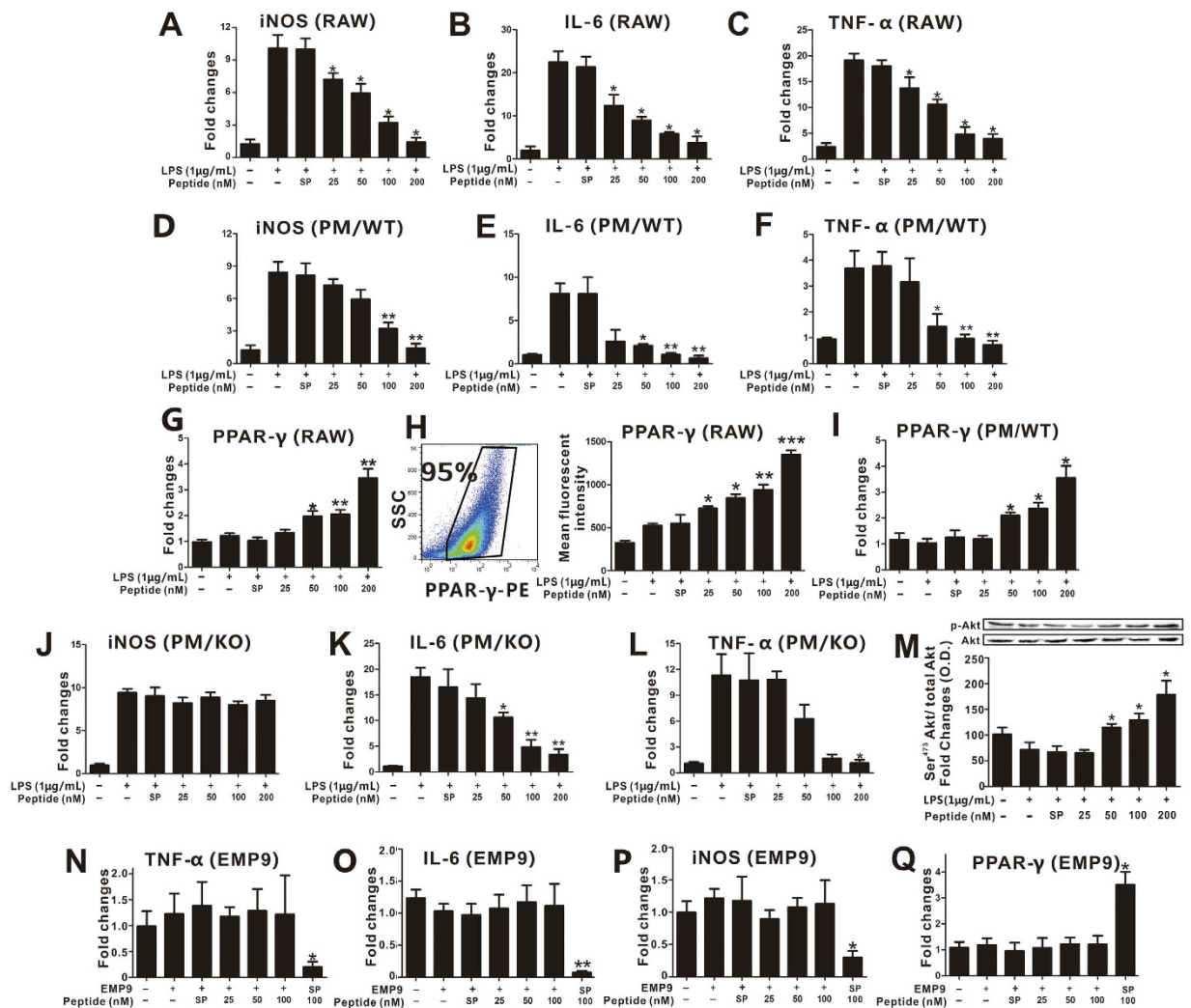


**Figure 3. pHBSP inhibits pro-inflammatory cytokine expression in macrophages *in vitro*.** (A–F) RAW 264.7 cells and peritoneal macrophages were treated with 1  $\mu\text{g}/\text{mL}$  LPS followed by various doses of pHBSP or PBS/scrambled peptide for 4 hours. pHBSP diminished the expression of iNOS (A), IL-6 (B) and TNF- $\alpha$  (C) mRNA in RAW264.7 cells and the expression of iNOS (D), IL-6 (E) and TNF- $\alpha$  (F) mRNA in peritoneal macrophages. (G–I) LPS-treated RAW 264.7 cells and peritoneal macrophages were subjected to various doses of pHBSP or PBS/scrambled peptide control and then the mRNA (G) and protein (H) levels of PPAR $\gamma$  in RAW264.7 cells and the mRNA levels of PPAR $\gamma$  (I) in peritoneal macrophages were measured by RT-PCR and flow cytometry, respectively. (J–L) Peritoneal macrophages were isolated from Mac-PPAR $\gamma$  knockout mice and were treated with 1  $\mu\text{g}/\text{mL}$  LPS followed by various doses of pHBSP or PBS/scrambled peptide for 4 hours. The expression of iNOS (J), IL-6 (K) and TNF- $\alpha$  (L) mRNA in PPAR $\gamma$  knockout macrophages was analyzed. (M) pHBSP increased Akt phosphorylation in LPS-treated RAW 264.7 cells. (N–Q) Administration of 0.5 mg/mL EMP9 counteracted the effects of pHBSP on the expression of TNF- $\alpha$  (M), IL-6 (N), iNOS (O) and PPAR $\gamma$  (P) mRNA in RAW264.7 cells. N = 3 per group; PM indicates peritoneal macrophages; SP indicates scrambled peptide; data are the mean  $\pm$  SEM; error bars indicate s.e.m., and significance is indicated by \* $p < 0.05$ , \*\* $p < 0.01$  and \*\*\* $p < 0.005$ , as determined by one-way analysis of variance followed by Dunnett's multiple comparison test.

Because fat mass gain is closely related to fatty acid oxidation, we examined the effects of pHBSP on fatty acid synthase gene (FASN) expression in WAT and Acox-1 expression in muscle and found that pHBSP decreased FASN (Fig. 5M,  $p < 0.05$ ) expression, whereas it increased Acox-1 (Fig. 5N,  $p < 0.05$ ) expression.

Because IR is an essential event towards metabolic dysregulation in obesity, we tested the levels of glucose and insulin tolerance following pHBSP treatment in DIO mice. pHBSP treatment normalized both glucose disposal rate (Fig. 6A,  $p < 0.05$ ) and insulin sensitivity (Fig. 6B,  $p < 0.05$ ). Furthermore,

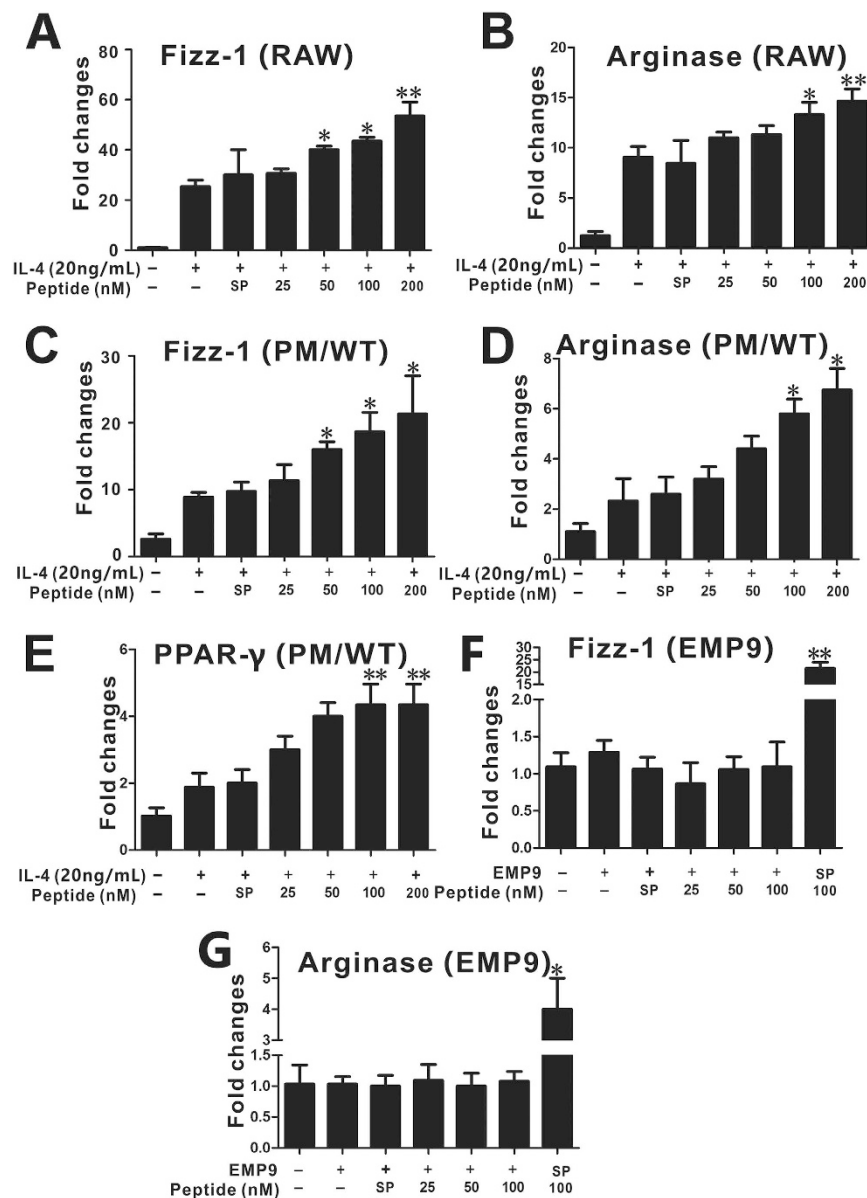


**Figure 4. pHBSP promotes M2 marker expression *in vitro*.** (A–E) RAW 264.7 cells and peritoneal macrophages were treated with 20 ng/mL IL-4 followed by various doses of pHBSP or PBS/scrambled peptide control for 24 hours. pHBSP increased the expression of Fizz-1 (A) and arginase-1 (B) mRNA in RAW264.7 cells and the expression of Fizz-1 (C), arginase-1 (D) and PPAR $\gamma$  (E) mRNA in peritoneal macrophages. (F,G) Administration of 0.5 mg/mL EMP9 counteracted the effects of pHBSP on the expression of Fizz-1 (F) and arginase-1 (G) mRNA in RAW264.7 cells. N = 3 per group; PM indicates peritoneal macrophages; SP indicates scrambled peptide; data are the mean  $\pm$  SEM; the error bars indicate s.e.m., and significance is indicated by \* $p < 0.05$  and \*\* $p < 0.01$ , as determined by one-way analysis of variance followed by Dunnett's multiple comparison test.

circulating triglyceride and total cholesterol levels in DIO mice were markedly attenuated by pHBSP (Fig. 6C,D,  $p < 0.05$ ).

In addition, we investigated whether pHBSP possessed hematopoietic properties during obesity treatment. Administration of pHBSP to HFD-fed mice every other day for 16 weeks did not alter spleen weight (Fig. 6E), the number of peripheral red blood cells (Fig. 6F), hemoglobin level (Fig. 6G) or hematocrit percentage (Fig. 6H), suggesting that pHBSP did not stimulate hematopoiesis during obesity treatment.

**pHBSP attenuates obesity-mediated inflammation and macrophage accumulation.** Given the important contribution of local inflammation to the development of IR in adipose tissue, we next

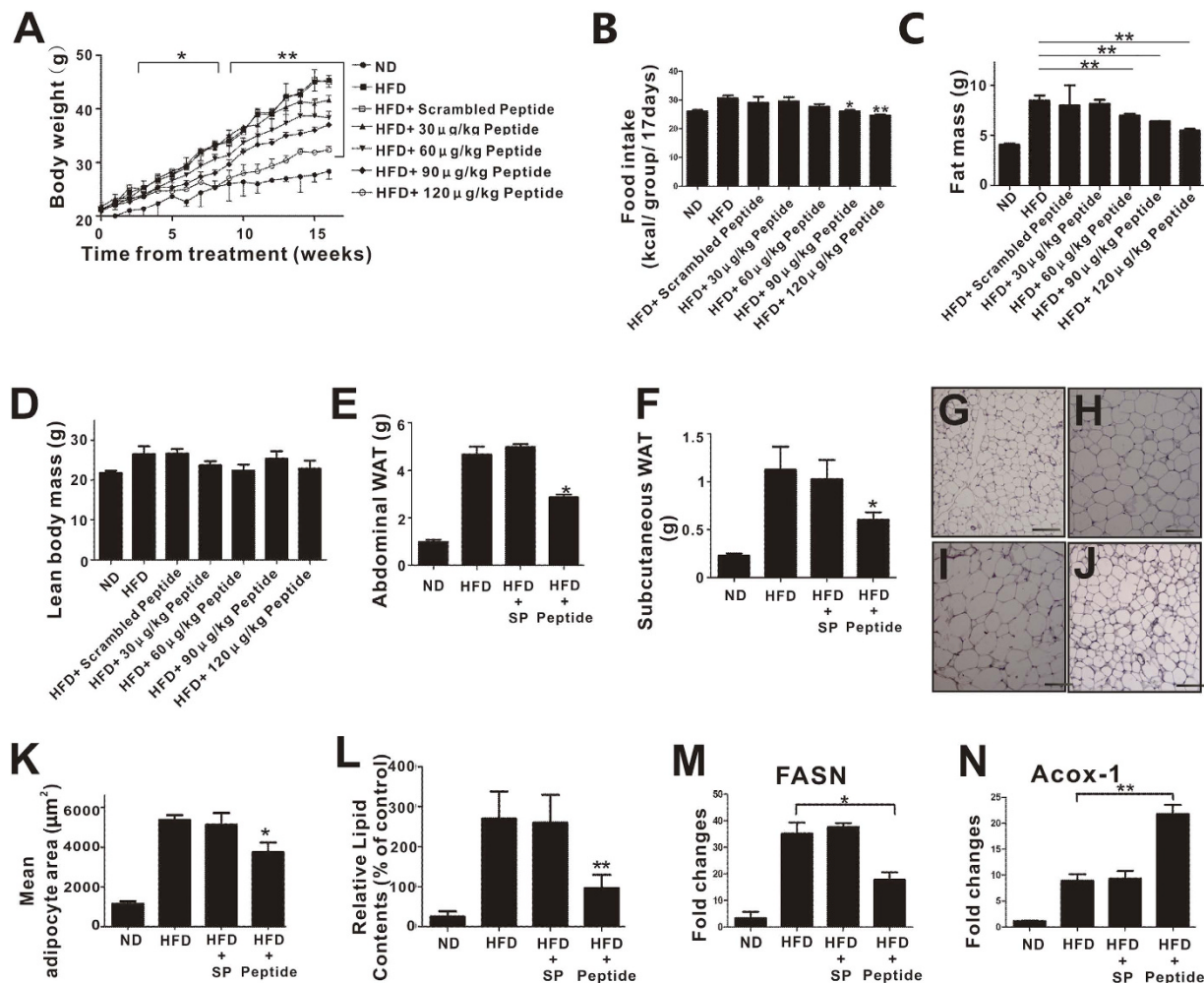


**Figure 5. pHBSP improves obesity.** C57BL/6 male mice (5–6 weeks of age) were put on an HFD and received exogenous pHBSP at different doses (30, 60, 90, and 120  $\mu$ g/kg). pHBSP was injected intraperitoneally using insulin syringes every other day. A subset of HFD-fed mice were injected with PBS/scrambled peptide only to serve as sham controls. (A–F) Body weight (A) and food intake (B) were measured once a week, and fat mass (C), lean mass (D), abdominal adipose (including mesenteric, retroperitoneal, and gonadal adipose) weight (E) and subcutaneous adipose weight (F) were measured when the mice were sacrificed at week 16. (G–K) Paratesticular WAT for H.E. staining was also performed after the mice were sacrificed at week 16. (G–J) shows representative H.E. staining of epididymal fat pad sections from ND-fed mice (G), HFD-fed mice (H), scrambled peptide-treated HFD-fed mice (I) or 120  $\mu$ g/kg pHBSP-treated HFD-fed mice (J). Bar graph shows the mean adipocyte area ( $\mu$ m<sup>2</sup>) (K). (L–N) 120  $\mu$ g/kg pHBSP decreased lipid storage in adipose tissue (L), decreased the expression of FASN (M) in WAT and increased Acox-1 expression in muscle (N). N = 6 per group; SP indicates scrambled peptide; Peptide indicates 120  $\mu$ g/kg pHBSP; data are the mean  $\pm$  SEM; the error bars indicate s.e.m., and significance is indicated by \* $p$  < 0.05 and \*\* $p$  < 0.01, as determined by Student's t-test. The scale bars are 100  $\mu$ m.

examined the expression of pro-inflammatory cytokines in epididymal WAT of HFD-fed mice and found that levels of TNF- $\alpha$ , IL-6, iNOS and MCP-1 were greatly reduced following pHBSP treatment for 16 weeks (Fig. 7A–D,  $p$  < 0.05).

Because macrophages play dominant roles in obesity-associated inflammation, we next examined whether pHBSP affected ATMs in HFD-fed mice. First, we found that pHBSP treatment dramatically reduced the accumulation of F4/80<sup>+</sup> macrophage clusters (CLSs) in epididymal fat pads (Fig. 7E–H). Then, we measured the expression of certain cytokines in ATMs following pHBSP treatment. Epididymal fat pad stromal vascular cells (SVF) were isolated, and the mRNA levels of different cytokines were analyzed. pHBSP administration decreased levels of TNF- $\alpha$ , IL-6 and iNOS, whereas it increased the expression of M2 macrophage-related molecules, such as Fizz-1 and Arginase-1, in the SVF of HFD-fed

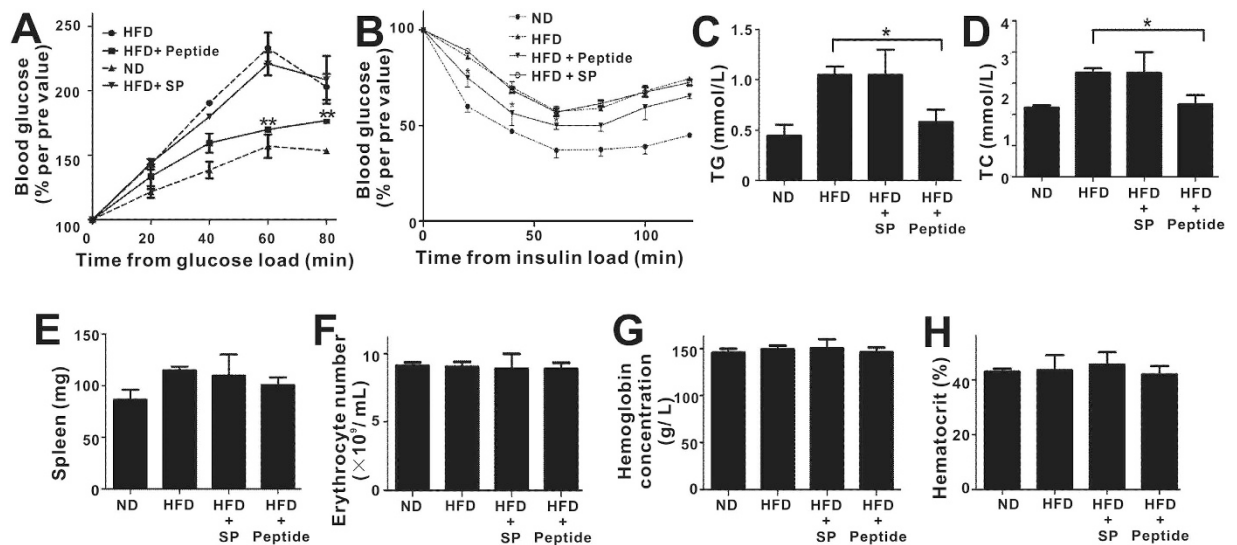


**Figure 6. pHBSP improves insulin resistance but does not stimulate hematopoiesis.** C57BL/6 male mice (5–6 weeks of age) were put on an HFD and received exogenous pHBSP at different doses (30, 60, 90, and 120  $\mu\text{g}/\text{kg}$ ). pHBSP was injected intraperitoneally using insulin syringes every other day. A subset of HFD-fed mice were injected with PBS/scrambled peptide to serve as a sham control. (A,B) Glucose and insulin tolerance tests were performed at week 16 on ND-fed mice, HFD-fed mice, scrambled peptide-treated HFD-fed mice and 120  $\mu\text{g}/\text{kg}$  peptide-treated HFD-fed mice. (C,D) At week 16, the mice in each group were sacrificed to take peripheral blood for detection of blood triglyceride and total cholesterol levels. Treatment with 120  $\mu\text{g}/\text{kg}$  pHBSP attenuated circulating triglyceride (C) and total cholesterol (D) levels in HFD-fed mice. (E–H) At week 16, the mice were sacrificed for spleen and peripheral blood harvest for the detection of erythropoietic activation. (E–H) show spleen weight measurements (E), peripheral red blood cell numbers (F), hemoglobin levels (G) and hematocrit percentage (H) in each group.  $N = 6$  per group; SP indicates scrambled peptide; Peptide indicates 120  $\mu\text{g}/\text{kg}$  pHBSP; data are the mean  $\pm$  SEM; the error bars indicate s.e.m., and significance is indicated by \* $p < 0.05$  and \*\* $p < 0.01$ .

mice (Fig. 7I–M,  $p < 0.01$ ). Furthermore, pHBSP significantly increased PPAR $\gamma$  expression in F4/80 $^+$  ATMs from the SVF of HFD-fed mice (Fig. 7N,  $p < 0.05$ ).

## Discussion

Growing attention has focused on the nonerythropoietic activity of EPO, such as its role in obesity regulation<sup>38</sup>. It has been reported that EPO reduces food intake and preadipocyte differentiation and increases fat oxidation, leading to improved fat mass and IR in DIO mice<sup>24,39–41</sup>. However, safety concerns have been raised over long-term and high-dose application of EPO, which has been associated with hypertension and thrombosis<sup>25</sup>. The EPO analogue pHBSP was reported to retain the tissue-protective functions of EPO but without its erythropoietic properties<sup>26</sup>. Specifically, Collino *et al.* reported that chronic treatment with pHBSP improved metabolic abnormalities induced by HFD<sup>42</sup>. Furthermore, in the clinic, pHBSP was demonstrated to improve metabolic indexes in patients suffering from type 2 diabetes<sup>43</sup>. Although these studies are exciting and provide the first strong evidence to support further investigations of pHBSP effects on obesity and related disorders, several important issues have been left unanswered from these studies, such as whether pHBSP can effectively prevent the development of obesity, what the dose-response of pHBSP is in obese individuals and, more importantly, whether other mechanisms exist regarding the effects of pHBSP on obesity modulation. Our current results show that preventive treatment with pHBSP significantly reduced weight gain and improved IR, suggesting a preventive effect of pHBSP in obesity modulation. Moreover, pHBSP was observed to have a dose-dependent effect, ranging from 30 to 120  $\mu\text{g}/\text{kg}$ , in obesity modulation, providing evidence for a wider dose choice. Mechanistically, unlike Collino's research, which mainly focused on skeletal muscle, our research revealed the anti-inflammatory and anti-adipogenesis effects of pHBSP peptide on adipocytes and macrophages, suggesting that this peptide may improve obesity through multiple mechanisms and target cells. Therefore, together with Collino's report, our current investigations prove that pHBSP has protective effects in obesity modulation and support the application of pHBSP in treating obesity.

Obesity is associated with hyperplasia and hypertrophy of adipocytes in white adipose tissue, the main site for excess energy storage<sup>44</sup>. Increased adipose tissue mass may result from increased sizes and numbers of adipocytes, which principally reflects the amount of stored triglycerides<sup>14</sup>. Therefore, reducing adipocyte hyperplasia and/or hypertrophy would be of benefit in obesity treatment. In this study, mice fed



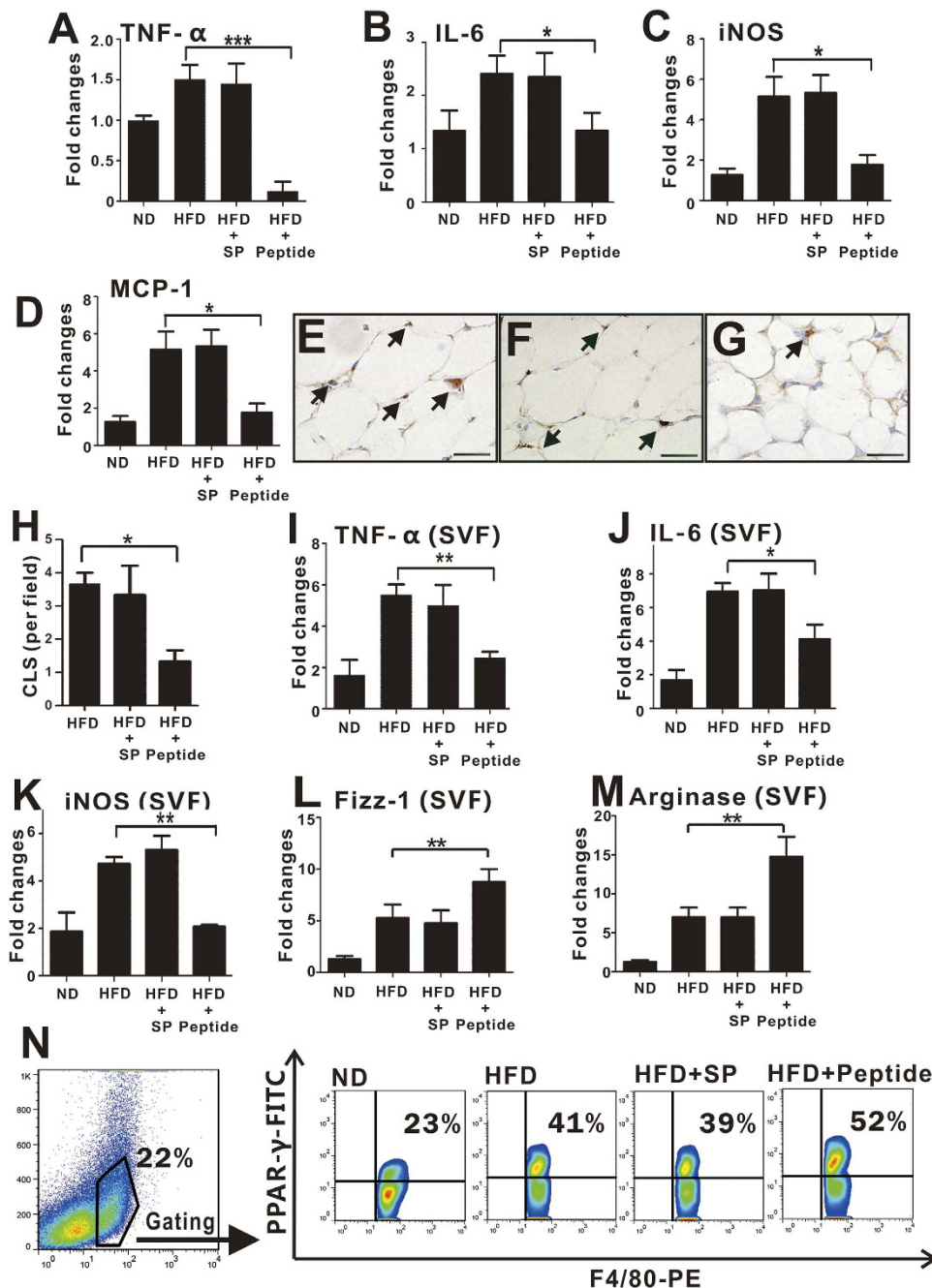


**Figure 7. pHBSP attenuates inflammation *in vivo*.** (A–D) PBS, scrambled peptide or pHBSP (120  $\mu$ g/kg/2days) was given to HFD-fed mice, and ND-fed mice were injected with PBS as a sham control. At week 16, the mice were sacrificed to take WAT for RT-PCR. (A–D) The expression of TNF- $\alpha$  (A), IL-6 (B), iNOS (C) and MCP-1 (D) in WAT decreased following 120  $\mu$ g/kg pHBSP treatment compared with the control group. (E–H) F4/80 staining was applied to visualize ATM infiltration in the adipose tissue taken at week 16. The arrows indicate CLS formation in adipose tissue in HFD-fed mice treated with PBS, 120  $\mu$ g/kg scrambled peptide or 120  $\mu$ g/kg pHBSP. ATM (F4/80<sup>+</sup>) infiltration was significantly suppressed by 120  $\mu$ g/kg pHBSP treatment compared to PBS and scrambled peptide control treatment (n = 6). (I–M) SVF cells were isolated from adipose tissue at week 16, and 120  $\mu$ g/kg pHBSP diminished the expression of TNF- $\alpha$  (I), IL-6 (J) and iNOS (K) mRNA in SVF cells, whereas the treatment up-regulated the expression of Fizz-1 (L) and arginase-1 (M) mRNA. (N) The mice were sacrificed at week 16 to harvest SVF cells from adipose tissue, and the protein levels of PPAR $\gamma$  in F4/80<sup>+</sup> SVF cells were measured. Treatment with 120  $\mu$ g/kg pHBSP increased PPAR $\gamma$  expression in F4/80<sup>+</sup> SVF. N = 6 per group; SVF indicates stromal vascular fraction; SP indicates scrambled peptide; Peptide indicates 120  $\mu$ g/kg pHBSP; data are the mean  $\pm$  SEM; the error bars indicate s.e.m., and significance is indicated by \*p < 0.05, \*\*p < 0.01 and \*\*\*p < 0.005, as determined by one-way analysis of variance followed by Dunnett's multiple comparison test. The scale bars are 50  $\mu$ m.

an HFD suffered from increased fat mass, higher levels of blood triglycerides and expanded adipocytes. Notably, pHBSP intervention significantly reduced food intake, fat mass, adipocyte size, and triglyceride synthesis/storage in both adipose tissue and adipocytes. Furthermore, pHBSP blocked 3T3-L1 preadipocyte MCE. These data are consistent with previous studies documenting the effect of EPO on obesity<sup>45</sup>. In addition, we discovered that pHBSP can down-regulate FASN in WAT while promoting Acox-1 expression in muscle. FASN is a well-known rate-limiting enzyme in fatty acid synthesis, and in addition to being rate-limiting Acox-1 is the first enzyme in the fatty acid beta-oxidation pathway<sup>46</sup>. This suggests that pHBSP can inhibit fatty acid synthesis and promote fatty acid oxidation, which may be another potential mechanism behind pHBSP's suppression of body weight and fat accumulation in obesity.

Obesity increases the risk for T2D by inducing IR. Although the manner in which obesity influences IR is not fully known, over the past several years, the significant contributions of pro-inflammatory molecules, such as TNF- $\alpha$ , IL-6, iNOS and MCP-1, to IR have been elucidated<sup>14</sup>. The deletion of TNF- $\alpha$  has been found to ameliorate inflammation and IR in DIO, and treatment with antibodies against TNF- $\alpha$  can increase insulin sensitivity in muscle<sup>47,48</sup>. IL-6 can reduce insulin-dependent hepatic glycogen synthesis and glucose uptake in adipocytes, whereas it enhances insulin-dependent glycogen synthesis and glucose uptake in myotubes<sup>49</sup>. MCP-1 contributes to macrophage infiltration in adipose tissue<sup>50</sup>. Macrophages and adipocytes are the main source of these molecules in obesity. In the current study, pHBSP ameliorated IR in obese mice and, notably, suppressed the expression of TNF- $\alpha$ , IL-6, iNOS and MCP-1 in both adipocytes and macrophages, indicating that pHBSP may improve IR through suppressing the inflammatory activation of macrophages and adipocytes.

Mechanistically, our study revealed that pHBSP significantly inhibited PPAR $\gamma$  expression in 3T3-L1 preadipocytes. PPAR $\gamma$  is a master regulator of adipogenesis, and down-regulation of PPAR $\gamma$  in adipocytes decreases fat mass<sup>51</sup>. Moreover, PPAR $\gamma$  knockout mice completely lack adipose tissue<sup>52</sup>. In addition, adipocyte differentiation is dependent on PPAR $\gamma$ , and the activation of PPAR $\gamma$  results in increased gene expression of adipogenic markers, such as fatty acid synthase<sup>51</sup>. Moreover, PPAR $\gamma$  also affects the expression of IR-related adipokines, such as TNF- $\alpha$ , IL-6 and MCP-1, in adipocytes<sup>53</sup>. Therefore, given the important roles that PPAR $\gamma$  plays in adipocytes, it is reasonable to speculate that pHBSP may at least partly inhibit adipogenesis and inflammatory cytokine expression in adipocytes through the down-regulation of PPAR $\gamma$  expression.

Conversely, we discovered that pHBSP induced PPAR $\gamma$  expression in macrophages. Accumulated data have shown that PPAR $\gamma$  is a ligand-dependent nuclear receptor, which has potentially anti-inflammatory effects in macrophages. The macrophage-specific deletion of PPAR $\gamma$  leads to an increase in local inflammation in adipose tissue, characterized by decreased expression of TNF- $\alpha$ , IL-6 and iNOS. On the contrary, the PPAR $\gamma$  agonist TZD can inhibit the production of inflammatory cytokines in macrophages<sup>54–56</sup>. Using PPAR $\gamma$  knockout macrophages, we found that pHBSP reduced iNOS expression, but not TNF- $\alpha$  and IL-6 expression, via PPAR $\gamma$ , indicating the existence of other signaling pathways for pHBSP-related anti-inflammatory effects. Previous investigations have shown that EPO inhibits the expression of TNF- $\alpha$  and IL-6 by suppressing Nuclear Factor- $\kappa$ B (NF $\kappa$ B) activation in macrophages<sup>37</sup>, suggesting that the EPO-derived pHBSP might inhibit NF $\kappa$ B activation as well. Therefore, these data suggest that pHBSP may suppress inflammatory macrophage activation through multiple signaling pathways, leading to increased PPAR $\gamma$  expression and decreased NF $\kappa$ B activation.

Although the manner in which PPAR $\gamma$  is differently regulated by pHBSP in adipocytes and macrophages remains elusive, previous EPO studies may provide some clues. It has been reported that EPO activates ERK, which further increased PPAR $\gamma$  phosphorylation and decreased PPAR $\gamma$  activity in 3T3-L1 cells<sup>58</sup>. However, in macrophages, the activation of the ERK pathway by EPO increased the expression of C/EBP $\beta$ , a transcriptional activator for PPAR $\gamma$ <sup>59,60</sup>, leading to the up-regulation of PPAR $\gamma$ . Therefore, pHBSP may modulate PPAR $\gamma$  expression differently through different signal pathways in adipocytes and macrophages.

In summary, the protective role of pHBSP in obesity and IR was established in the current study. pHBSP may be a promising candidate for DIO intervention, improving IR and attenuating inflammation through multiple mechanisms.

## Methods

All animal care and experiments were approved by the Animal Care and Use Committees of Third Military Medical University. All methods were carried out in accordance with the approved guidelines.

**3T3-L1 cell culture and adipocyte differentiation.** For 3T3-L1 cell culture, 3T3-L1 preadipocytes were first grown in complete DMEM (Gibco, Grand Island, NY, USA) with 10% bovine calf serum at 37°C and 5% CO<sub>2</sub> until 3 days post-confluence. Next, the confluent cells were incubated in complete DMEM containing 10% FBS (Gibco, Grand Island, NY, USA), 1  $\mu$ M dexamethasone, 0.5 mM isobutylmethylxanthine and 5  $\mu$ g/mL insulin at 37°C and 5% CO<sub>2</sub> for 2 days. Then, the medium was replaced with complete DMEM with 10% FBS and 5  $\mu$ g/mL insulin for another 2 days. Finally, the medium was replaced with complete DMEM containing 10% FBS (with different doses of pHBSP or PBS/scrambled peptide control), with the medium being replaced every 2 days.

In order to keep the comparability of the whole study, we set both PBS and scrambled peptide as control.

**ORO staining.** Mature adipocytes were fixed with 10% formalin for 1 minute. Then, the formalin was removed, and the cells were stained with ORO solution (Sigma-Aldrich) and washed with PBS. For quantification, the ORO was re-suspended in isopropyl alcohol, and the absorbance was measured spectrophotometrically at 515 nm.

**Isolation of mouse peritoneal macrophages, and cell model establishment, culture and treatment.** To isolate mouse peritoneal macrophages, a peritoneal lavage with 20 mL DMEM containing 2% FBS and 100 units/mL penicillin was applied. After centrifugation (1000 rpm, 5 min), red blood cells were lysed in Red Blood Cell Lysis Buffer (Biolegend, San Diego, CA, USA), and mononuclear cells were plated and maintained in complete DMEM containing 10% FBS, 100 units/mL penicillin and 100 units/mL streptomycin at 37°C for 2 h. Then, non-adherent cells were removed, and the remaining adherent cells were cultured in complete DMEM with 10% FBS.

For RAW264.7 cell culture, the cells were grown in complete DMEM with 10% fetal calf serum, 100 units/mL penicillin and 100 units/mL streptomycin at 37°C and 5% CO<sub>2</sub>.

For the M1/M2 model, macrophages were induced with 1 µg/mL LPS for 8 h or 20 ng/mL IL-4 for 24 h, together with different doses of pHBSP (synthesized by Chinesepeptide Corporation, Hangzhou, China, sequence: QEQLERALNSS; purity: 98%) or PBS/200 nM scrambled peptide.

It has been reported that TPR consists of EPOR and βcR subunits<sup>42</sup>. To inhibit TPR function, erythropoietin mimetic peptide-9 (EMP-9), a proven EPOR antagonist, was applied. The EMP-9 was dissolved in complete DMEM to a final concentration of 0.5 mg/mL.

**Animals and pHBSP intervention.** Male C57BL/6 mice (5–6 weeks old, Vital River, Beijing, China) were fed either a standard maintenance diet (normal chow, 2844 kcal/kg, 4% crude fat, Daping Hospital, Chongqing, China) or an HFD containing 5240 kcal/kg (high fat, 34.9% crude fat, Daping Hospital, Chongqing, China). All animals in this study were subject to controlled temperature (22 ± 1°C) and lighting (lights on 06:00 to 18:00) conditions. All animal experimental procedures were subject to approval by the Animal Care and Use Committees of Third Military Medical University. All efforts were made to minimize the number of animals used and their suffering.

The mice were separated randomly into distinct groups based on pHBSP dose (n = 6 mice/group, doses were 30, 60, 90, and 120 µg/kg); the doses of pHBSP were based on our former study, which showed the therapeutic effect of the long-term use of pHBSP on experimental autoimmune neuritis<sup>33</sup>. The interval of pHBSP administration was based on previous clinical data that demonstrated that the repetitive administration of pHBSP was effective despite its short half-life<sup>34</sup>. The pHBSP was dissolved in PBS. An equivalent volume of PBS and 120 µg/kg scrambled peptide was used as a control group. The PBS and peptide mixture were administered intraperitoneally using insulin syringes (B. Braun Melsungen AG, Germany) every other day.

**Body weight and fat mass measurement.** The mice were individually weighed weekly. At week 16, they were sacrificed by cervical dislocation. Next, subcutaneous fat deposits were dissected and weighted. Then, abdominal fat deposits (including fat pads associated with the epididymis, kidneys and mesentery) were isolated and weighted. Together, the subcutaneous and abdominal fat mass constituted the fat mass, and the body mass minus the cleared out fat mass constituted the lean body mass.

**Glucose and insulin tolerance tests.** Mice (n = 6/group) were fasted for 16 hours and challenged with 1) an intraperitoneal load of glucose (1 g/kg) for glucose tolerance testing, or 2) an intraperitoneal load of human insulin (0.375 IU/kg, Actrapid, Novo Nordic, Denmark) for insulin tolerance testing. Blood samples (10 µL) were taken retro-orbitally from conscious mice at 0, 30, 60, 90, 120, and 180 min after glucose or insulin load. Blood glucose levels were determined with the help of a Onetouch Ultra (Johnson & Johnson, USA).

**Epididymal fat pad SVF isolation and ATM purification.** First, epididymal fat pads from each group were collected and collagenase (Sigma-Aldrich, 1 mg/mL) was added and incubated at 37°C for 80 minutes with shaking. Next, the resultant cell suspensions were filtered through 70-µm filters. After centrifugation (300 g, 5 min), floating mature adipocytes were removed. Then, the cells were plated and cultured in complete DMEM containing 10% FBS, 100 units/mL penicillin and 100 units/mL streptomycin at 37°C for 2 h. Following this, non-adherent cells were removed, and the remaining adherent cells were analyzed.

**Flow cytometry.** Single-cell suspensions from SVF, 3T3-L1 cells, and macrophages were washed twice in staining buffer, re-suspended, and incubated with labeled antibodies at 4°C for 30 min. After that, the cells were washed twice with staining buffer and analyzed. F4/80 and PPARγ staining was performed as per manufacturer's instructions (Sungene Biotech, Tianjin, China).

For cell cycle analysis, two days post-confluence, 3T3-L1 preadipocytes were induced to differentiate with different doses of pHBSP or PBS/scrambled peptide. Twenty-four hours later, the cells were harvested and fixed with 75% ethanol for 12 h at 4°C. Then, the ethanol was removed, and the cells were

Primers	Sequences
FASN forward	GGACATGGTCACAGACGATGAC
FASN reverse	GTCGAACTGGACAGATCCTTCA
Leptin forward	TCCAGAAAGTCCAGGATGACAC
Leptin reverse	CACATTTTGGGAAGGCAGG
Adiponectin forward	AAGGACAAGGCCGTTCTCT
Adiponectin reverse	TATGGGTAGTTGCAGTCAGTTGG
PPAR $\gamma$ forward	GGAATGGGAGTGGTCATCCA
PPAR $\gamma$ reverse	CCCACCAACTTCGGAATC
TNF- $\alpha$ forward	CGTCAGCCGATTGCTATCT
TNF- $\alpha$ reverse	CGGACTCCGCAAAGTCTAAG
IL-6 forward	ACAAGTCGGAGGCTTAATTAC
IL-6 reverse	TTGCCATTGCACAACTCTTTC
iNOS forward	AATGGCAACATCAGGTCGGCCATCACT
iNOS reverse	GCTGTGTGTACAGAAGTCTCGAACTC
MCP-1 forward	CTTCTCCACCACCATGC
Fizz-1 forward	TCCCAGTGAATACTGATGAGA
Fizz-1 reverse	CCACTCTGGATCTCCAAGA
Arginase forward	AAGCCTGGTCTGCTGGAAAAA
Arginase reverse	CTGGTTGTCAGGGGAGTGT
MCP-1 reverse	CCAGCCGGCAACTGTGA
$\beta$ -Actin forward	ATGGGTCAGAAGGACTCTACG
$\beta$ -Actin reverse	AGTGGTACGACCAGAGGCATAC

**Table 1. Sequences of primers for quantitative RT-PCR.**

washed twice with PBS and stained with propidium iodide solution containing 20  $\mu$ g/mL RNase for 30 min.

Flow cytometry analysis was performed on a Becton–Dickinson FACScan system, and the data were analyzed using FlowJo software (version 7.6.1, Tree Star Software, San Carlos, CA, USA).

**Western blot analysis.** For western blotting, the cells were washed twice with ice-cold PBS and lysed with cell lysis buffer (Beyotime, China) according to the manufacturer's protocol. Protein lysates were separated via 12% SDS-polyacrylamide gel electrophoresis for 1.5 h and transferred to a polyvinylidene difluoride membrane for 1 h. Then, the membrane was blocked with 5% non-fat milk for 1 h at 25  $^{\circ}$ C and incubated with primary antibodies against Akt and p-Akt (1:400, Santa Cruz, Texas, USA) at 4  $^{\circ}$ C overnight, followed by incubation with secondary antibodies (1:2000, Thermo Fisher, Waltham, MA, USA) conjugated to horseradish peroxidase for 1 h at 25  $^{\circ}$ C. Detection was performed using an ECL chemiluminescence kit (Millipore, Billerica, MA, USA), and the optical densities of phosphoprotein/total protein were analyzed using MyImage Analysis software (Thermo Fisher, Waltham, MA, USA).

**Tissue preparation, RNA isolation, reverse transcription and real-time PCR.** At week 16, the mice ( $n = 6$ /group) were perfused intracardially with 4  $^{\circ}$ C PBS under anesthesia, after which WAT were quickly removed and stored in liquid nitrogen until RNA isolation. Total RNA was isolated using Trizol LS reagent (Invitrogen, Carlsbad, CA, USA) and reverse transcribed into cDNA using a Quantscript RT Kit (TIANGEN Biotech, Beijing, China).

The cDNA was used to assess the relative expression of genes using RealMasterMix (SYBR green I) according to the manufacturer's protocol (TIANGEN Biotech, Beijing, China). Real-time measurements of gene expression were performed with a DNA Engine Opticon 2 Real-Time Cycler PCR detection system (Bio-Rad Lab., Richmond, CA, USA). The primers used to measure gene expression are described in Table 1.

**Histology.** To evaluate ATM accumulation, the mice were deeply anesthetized with ether and perfused intracardially with 4% paraformaldehyde at 4  $^{\circ}$ C in PBS. Epididymal fat pads were quickly removed and post-fixed in 4% paraformaldehyde overnight at 4  $^{\circ}$ C. The tissues were cut into two equally long segments, embedded in paraffin, serially sectioned (3  $\mu$ m) and mounted on silan-covered slides.

Routine hematoxylin and eosin (HE) staining was performed as described previously<sup>33</sup>. For immunohistochemistry, after dewaxing, cross-sections were boiled (in a 600 W microwave oven) for 15 min

in citrate buffer (2.1 g sodium citrate/L, pH 6). Endogenous peroxidase was inhibited with 1% H<sub>2</sub>O<sub>2</sub> in methanol for 15 minutes. The sections were incubated with 10% normal pig serum (Biochrom, Berlin, Germany) to block non-specific binding of immunoglobulins and then with an anti-mouse F4/80 antibody (1:50; Abcam, Cambridge, UK) for macrophage identification. Antibody binding to tissue sections was visualized with a biotinylated IgG F(ab)<sub>2</sub> secondary antibody fragment (DAKO, Hamburg, Germany). Subsequently, the sections were incubated with a horseradish peroxidase-conjugated streptavidin complex (DAKO, Hamburg, Germany) followed by development with diaminobenzidine (DAB) substrate (Fluka, Neu-Ulm, Germany). Finally, the sections were counterstained with Maier's Hemalum.

To evaluate the immunostaining data, CLSs were identified as adipocytes completely surrounded by F4/80<sup>+</sup> cells and were quantified in 6 random fields in all animals. Images of WAT cross-sections were collected under 50× magnification using a Nikon Coolscope (Nikon, Düsseldorf, Germany) with fixed parameters. The images were analyzed using MetaMorph Offline 7.1 (Molecular Devices, Toronto, Canada). The results are given as the numbers of CLSs per area in WAT cross-sections and include the standard errors of the means (SEM).

**Data evaluation and statistical analysis.** The data are expressed as mean ± s.e.m. Comparisons between two groups were made using two-tailed non-paired Student's t-test. Statistical differences between three or more groups were evaluated by one-way analysis of variance with Dunnett's multiple comparison post hoc tests at  $\alpha = 0.05$ . Area under the curve assessment was used in the glucose and insulin tolerance tests. A p value of <0.05 was considered to be statistically significant.

## References

- Vasilescu, R. & Ionescu-Tirgoviste, C. [Association of albuminuria with adipokines, inflammation and insulin resistance in non-diabetic subjects]. *Rev Med Chir Soc Med Nat Iasi* **115**, 1174–1182 (2011).
- Horowitz, J. F. & Klein, S. Whole body and abdominal lipolytic sensitivity to epinephrine is suppressed in upper body obese women. *Am J Physiol Endocrinol Metab* **278**, E1144–E1152 (2000).
- Guilherme, A., Virbasius, J. V., Puri, V. & Czech, M. P. Adipocyte dysfunctions linking obesity to insulin resistance and type 2 diabetes. *Nat Rev Mol Cell Biol* **9**, 367–377 (2008).
- Lubrano, C. *et al.* Obesity and metabolic comorbidities: environmental diseases? *OXID MED CELL LONGEV* **2013**, 640673 (2013).
- Obesity: preventing and managing the global epidemic. Report of a WHO consultation. *World Health Organ Tech Rep Ser* **894**, 1–253 (2000).
- Jo, J. *et al.* Hypertrophy and/or Hyperplasia: Dynamics of Adipose Tissue Growth. *PLOS COMPUT BIOL* **5**, e1000324 (2009).
- Spiegelman, B. M. & Flier, J. S. Adipogenesis and obesity: rounding out the big picture. *CELL* **87**, 377–389 (1996).
- Min, S. Y. *et al.* Cocoa polyphenols suppress adipogenesis *in vitro* and obesity *in vivo* by targeting insulin receptor. *Int J Obes (Lond)* **37**, 584–592 (2013).
- Xu, H. *et al.* Chronic inflammation in fat plays a crucial role in the development of obesity-related insulin resistance. *J CLIN INVEST* **112**, 1821–1830 (2003).
- Lumeng, C. N. & Saltiel, A. R. Inflammatory links between obesity and metabolic disease. *J CLIN INVEST* **121**, 2111–2117 (2011).
- Steinberg, G. R. *et al.* Tumor necrosis factor alpha-induced skeletal muscle insulin resistance involves suppression of AMP-kinase signaling. *CELL METAB* **4**, 465–474 (2006).
- Sartipy, P. & Loskutoff, D. J. Monocyte chemoattractant protein 1 in obesity and insulin resistance. *Proc Natl Acad Sci USA* **100**, 7265–7270 (2003).
- Bastarrachea, R. A. *et al.* [Macrophages, inflammation, adipose tissue, obesity and insulin resistance]. *GAC MED MEX* **143**, 505–512 (2007).
- Osborn, O. & Olefsky, J. M. The cellular and signaling networks linking the immune system and metabolism in disease. *NAT MED* **18**, 363–374 (2012).
- Hogan, A. E. *et al.* Glucagon-like peptide 1 analogue therapy directly modulates innate immune-mediated inflammation in individuals with type 2 diabetes mellitus. *DIABETOLOGIA* **57**, 781–784 (2014).
- Kolak, M., *et al.* Effects of chronic rosiglitazone therapy on gene expression in human adipose tissue *in vivo* in patients with type 2 diabetes. *J Clin Endocrinol Metab* **92**, 720–724 (2007).
- Premaratna, S. D. *et al.* Angiotensin-converting enzyme inhibition reverses diet-induced obesity, insulin resistance and inflammation in C57BL/6J mice. *Int J Obes (Lond)* **36**, 233–243 (2012).
- Krantz, S.B. Erythropoietin. *BLOOD* **77**, 419–434 (1991).
- Cokic, B. B., Cokic, V. P., Suresh, S., Wirt, S. & Noguchi, C. T. Nitric oxide and hypoxia stimulate erythropoietin receptor via MAPK kinase in endothelial cells. *MICROVASC RES* **92**, 34–40 (2014).
- Sargin, D. *et al.* Expression of constitutively active erythropoietin receptor in pyramidal neurons of cortex and hippocampus boosts higher cognitive functions in mice. *BMC BIOL* **9**, 27 (2011).
- Brines, M. & Cerami, A. Emerging biological roles for erythropoietin in the nervous system. *NAT REV NEUROSCI* **6**, 484–494 (2005).
- Hara, A. *et al.* Autoantibodies to erythropoietin receptor in patients with immune-mediated diseases: relationship to anaemia with erythroid hypoplasia. *Br J Haematol* **160**, 244–250 (2013).
- Wang, L. *et al.* PPARalpha and Sirt1 mediate erythropoietin action in increasing metabolic activity and browning of white adipocytes to protect against obesity and metabolic disorders. *DIABETES* **62**, 4122–4131 (2013).
- Teng, R. *et al.* Disrupted erythropoietin signalling promotes obesity and alters hypothalamus proopiomelanocortin production. *NAT COMMUN* **2**, 520 (2011).
- Jelkmann, W. Physiology and pharmacology of erythropoietin. *Transfus Med Hemother* **40**, 302–309 (2013).
- Brines, M., *et al.* Nonerythropoietic, tissue-protective peptides derived from the tertiary structure of erythropoietin. *Proc Natl Acad Sci USA* **105**, 10925–10930 (2008).
- Hand, C. C. & Brines, M. Promises and pitfalls in erythropoietin-mediated tissue protection: are nonerythropoietic derivatives a way forward? *J Investig Med* **59**, 1073–1082 (2011).
- Pulman, K. G., Smith, M., Mengozzi, M., Ghezzi, P. & Dille, A. The erythropoietin-derived peptide ARA290 reverses mechanical allodynia in the neuritis model. *NEUROSCIENCE* **233**, 174–183 (2013).

29. Collino, M., Thiemermann, C., Cerami, A. & Brines, M. Flipping the molecular switch for innate protection and repair of tissues: Long-lasting effects of a non-erythropoietic small peptide engineered from erythropoietin. *Pharmacol Ther* **151**, 32–40 (2015).
30. McVicar, C. M. *et al.* Intervention with an erythropoietin-derived peptide protects against neuroglial and vascular degeneration during diabetic retinopathy. *DIABETES* **60**, 2995–3005 (2011).
31. Zellinger, C. *et al.* Impact of the erythropoietin-derived peptide mimetic Epotris on the histopathological consequences of status epilepticus. *EPILEPSY RES* **96**, 241–249 (2011).
32. van Rijt, W. G. *et al.* ARA290, a non-erythropoietic EPO derivative, attenuates renal ischemia/reperfusion injury. *J TRANSL MED* **11**, 9 (2013).
33. Liu, Y., *et al.* Erythropoietin-derived nonerythropoietic peptide ameliorates experimental autoimmune neuritis by inflammation suppression and tissue protection. *PLOS ONE* **9**, e90942 (2014).
34. Heij, L. *et al.* Safety and efficacy of ARA 290 in sarcoidosis patients with symptoms of small fiber neuropathy: a randomized, double-blind pilot study. *MOL MED* **18**, 1430–1436 (2012).
35. Tang, Q. Q., Otto, T. C. & Lane, M. D. Mitotic clonal expansion: a synchronous process required for adipogenesis. *Proc Natl Acad Sci USA* **100**, 44–49 (2003).
36. Cong, L. N. *et al.* Physiological role of Akt in insulin-stimulated translocation of GLUT4 in transfected rat adipose cells. *MOL ENDOCRINOL* **11**, 1881–1890 (1997).
37. Yasuda, Y. *et al.* Erythropoietin regulates tumour growth of human malignancies. *CARCINOGENESIS* **24**, 1021–1029 (2003).
38. Alnaeeli, M. *et al.* Erythropoietin signaling: a novel regulator of white adipose tissue inflammation during diet-induced obesity. *DIABETES* **63**, 2415–2431 (2014).
39. Foskett, A., Alnaeeli, M., Wang, L., Teng, R. & Noguchi, C. T. The effects of erythropoietin dose titration during high-fat diet-induced obesity. *J Biomed Biotechnol* **2011**, 373781 (2011).
40. Hojman, P., *et al.* Erythropoietin over-expression protects against diet-induced obesity in mice through increased fat oxidation in muscles. *PLOS ONE* **4**, e5894 (2009).
41. Sanchis-Gomar, F. *et al.* Erythropoietin and the heart: physiological effects and the therapeutic perspective. *INT J CARDIOL* **171**, 116–125 (2014).
42. Collino, M. *et al.* A non-erythropoietic peptide derivative of erythropoietin decreases susceptibility to diet-induced insulin resistance in mice. *Br J Pharmacol* **171**, 5802–5815 (2014).
43. Brines, M. *et al.* ARA 290, a Nonerythropoietic Peptide Engineered from Erythropoietin, Improves Metabolic Control and Neuropathic Symptoms in Patients with Type 2 Diabetes. *MOL MED* **20**, 658–666 (2015).
44. Loftus, T. M. *et al.* Reduced food intake and body weight in mice treated with fatty acid synthase inhibitors. *SCIENCE* **288**, 2379–2381 (2000).
45. Mikolas, E. *et al.* Effects of erythropoietin on glucose metabolism. *HORM METAB RES* **44**, 279–285 (2012).
46. Kwon, H. & Pessin, J. E. Adipokines mediate inflammation and insulin resistance. *Front Endocrinol (Lausanne)* **4**, 71 (2013).
47. Peraldi, P., Xu, M. & Spiegelman, B. M. Thiazolidinediones block tumor necrosis factor- $\alpha$ -induced inhibition of insulin signaling. *J CLIN INVEST* **100**, 1863–1869 (1997).
48. Uysal, K. T., Wiesbrock, S. M., Marino, M. W. & Hotamisligil, G. S. Protection from obesity-induced insulin resistance in mice lacking TNF- $\alpha$  function. *NATURE* **389**, 610–614 (1997).
49. Lagathu, C. *et al.* Chronic interleukin-6 (IL-6) treatment increased IL-6 secretion and induced insulin resistance in adipocyte: prevention by rosiglitazone. *Biochem Biophys Res Commun* **311**, 372–379 (2003).
50. Kanda, H. *et al.* MCP-1 contributes to macrophage infiltration into adipose tissue, insulin resistance, and hepatic steatosis in obesity. *J CLIN INVEST* **116**, 1494–1505 (2006).
51. Kubota, N. *et al.* PPAR  $\gamma$  mediates high-fat diet-induced adipocyte hypertrophy and insulin resistance. *MOL CELL* **4**, 597–609 (1999).
52. Miles, P. D., Barak, Y., He, W., Evans, R. M. & Olefsky, J. M. Improved insulin-sensitivity in mice heterozygous for PPAR- $\gamma$  deficiency. *J CLIN INVEST* **105**, 287–292 (2000).
53. Ahmadian, M. *et al.* PPAR $\gamma$  signaling and metabolism: the good, the bad and the future. *NAT MED* **19**, 557–566 (2013).
54. Chawla, A. *et al.* PPAR- $\gamma$  dependent and independent effects on macrophage-gene expression in lipid metabolism and inflammation. *NAT MED* **7**, 48–52 (2001).
55. Neri, T. *et al.* Effects of peroxisome proliferator-activated receptor- $\gamma$  agonists on the generation of microparticles by monocytes/macrophages. *CARDIOVASC RES* **94**, 537–544 (2012).
56. Hu, E., Kim, J. B., Sarraf, P. & Spiegelman, B. M. Inhibition of adipogenesis through MAP kinase-mediated phosphorylation of PPAR $\gamma$ . *SCIENCE* **274**, 2100–2103 (1996).
57. Nairz, M. *et al.* Erythropoietin contrastingly affects bacterial infection and experimental colitis by inhibiting nuclear factor- $\kappa$ B-inducible immune pathways. *IMMUNITY* **34**, 61–74 (2011).
58. Hu, J. *et al.* ERK1 and ERK2 activate CCAAAT/enhancer-binding protein- $\beta$ -dependent gene transcription in response to interferon- $\gamma$ . *J BIOL CHEM* **276**, 287–297 (2001).
59. Nonami, A. *et al.* Spred-1 negatively regulates interleukin-3-mediated ERK/mitogen-activated protein (MAP) kinase activation in hematopoietic cells. *J BIOL CHEM* **279**, 52543–52551 (2004).
60. Prusty, D., Park, B. H., Davis, K. E. & Farmer, S. R. Activation of MEK/ERK signaling promotes adipogenesis by enhancing peroxisome proliferator-activated receptor  $\gamma$  (PPAR $\gamma$ ) and C/EBP $\alpha$  gene expression during the differentiation of 3T3-L1 preadipocytes. *J BIOL CHEM* **277**, 46226–46232 (2002).

## Acknowledgements

This investigation was supported by the National Science and Technology Major Projects of New Drugs (2012ZX09103301-035).

## Author Contributions

Conceived and designed experiments: Z.R. Performed experiments: Y.L., B.L., R.S., J.W. and Z.L. Assess the data: Y.L., B.L., W.L. and S.W. Contributed reagents/materials/analysis tools: Z.R. and W.L. Wrote the paper: Y.L. Revised the paper: Z.R.

## Additional Information

**Supplementary information** accompanies this paper at <http://www.nature.com/srep>

**Competing financial interests:** The authors declare no competing financial interests.

**How to cite this article:** Liu, Y. *et al.* Nonerythropoietic Erythropoietin-Derived Peptide Suppresses Adipogenesis, Inflammation, Obesity and Insulin Resistance. *Sci. Rep.* **5**, 15134; doi: 10.1038/srep15134 (2015).



This work is licensed under a Creative Commons Attribution 4.0 International License. The images or other third party material in this article are included in the article's Creative Commons license, unless indicated otherwise in the credit line; if the material is not included under the Creative Commons license, users will need to obtain permission from the license holder to reproduce the material. To view a copy of this license, visit <http://creativecommons.org/licenses/by/4.0/>